Backbone-Branched DNA Building Blocks for Facile Angular Control in Nanostructures

Eduardo Paredes,[†] Xiaojuan Zhang,[‡] Harshad Ghodke,[§] Vamsi K. Yadavalli,[‡,*] and Subha R. Das[†,*]

[†]Department of Chemistry and Center for Nucleic Acids Science and Technology, Carnegie Mellon University. 4400 Fifth Avenue, Pittsburgh, Pennsylvania 15213, United States, [‡]Department of Chemical & Life Science Engineering. Virginia Commonwealth University, 601 West Main Street, Richmond, Virginia 23284, United States, and [§]Department of Pharmacology & Chemical Biology. University of Pittsburgh Medical Center, 5117 Centre Avenue, Pittsburgh, Pennsylvania 15213, United States

ABSTRACT

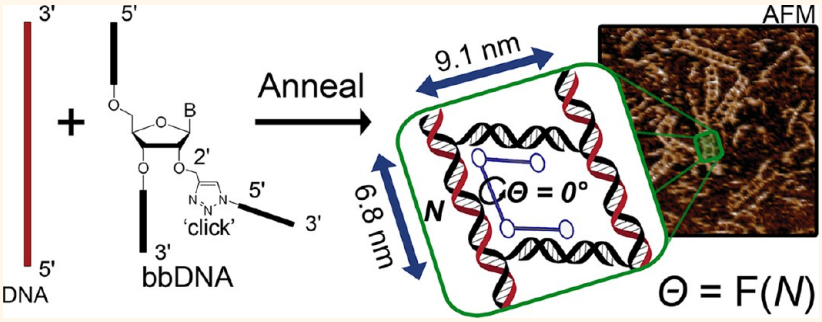

Nanotechnology based on the highly specific pairing of nucleobases in DNA has been used to generate a wide variety of well-defined two- and three-dimensional assemblies, both static and dynamic. However, control over the junction angles to achieve them has been limited. To achieve higher order assemblies, the strands of the DNA duplex are typically made to deviate at junctions with configurations based on crossovers or non-DNA moieties. Such strand crossovers tend to be intrinsically unstructured with the overall structural rigidity determined by the architecture of the nanoassembly, rather than the junction itself. Specific approaches to define nanoassembly junction angles are based either on the cooperative twist- and strain-promoted tuning of DNA persistence length leading to bent DNA rods for fairly large nano-objects, or *de novo* synthesis of individual junction inserts that are typically non-DNA and based on small organic molecules or metal-coordinating ligand moieties. Here, we describe a general strategy for direct control of junction angles in DNA nanostructures that are completely tunable about the DNA helix. This approach is used to define angular vertices through readily accessible backbone-branched DNAs (bbDNAs). We demonstrate how such bbDNAs can be used as a new building block in DNA nanoconstruction to obtain well-defined nanostructures. Angular control through readily accessible bbDNA building block provides a general and versatile approach for incorporating well-defined junctions in nanoconstructs and expands the toolkit toward achieving strain free, highly size- and shape-tunable DNA based architectures.

KEYWORDS: DNA nanostructures · backbone-branched DNA · click chemistry · nanoassembly · junction angles

The crux of DNA nanotechnology lies in the precise control and self-assembly of DNA into organized functional materials. Pioneering work on immobile Holliday junctions,[1,2] the basis of more elaborate assemblies, established DNA not only as a functional biomacromolecule, but a versatile material for nanoconstruction.[3−7] Since then, DNA origami[8] and methods that facilitate twists and bends have provided routes to assembling complex 2D and 3D structures.[9−25] Such nano-objects are now being exploited for applications in imaging and biological delivery.[26−29] Although such successes are prominent, they have also underscored the limitations in angular control in DNA assemblies leading to complex shapes and patterns.

The Holliday junction, three way junction (3WJ) and related antiparallel double crossover motifs that typically form the basis of DNA nanostructures tend to be inherently unstructured. Recent high resolution structural analyses have shown that even in a

* Address correspondence to srdas@andrew.cmu.edu, vyadavalli@vcu.edu.

Received for review December 16, 2012 and accepted April 19, 2013.

Published online April 19, 2013
10.1021/nn305787m

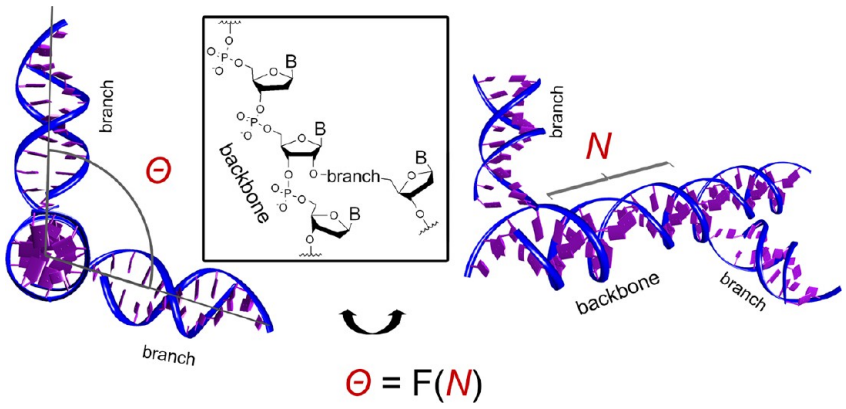

Figure 1. A general schematic for direct angular control in DNA nanoassemblies. Given the periodic helicity of the B-form DNA duplex, the dihedral angle (Θ) between branches emanating from the sugar−phosphate backbone (inset) is proportional to the number of residues (*N*) *between* the branches. As the branchpoint is on the backbone, the bases of the branch can hybridize in duplexes. DNA structure adapted from B-form DNA duplex PDBID: 1BDNA.

fully complementary 3WJ, the bases adjacent to the crossover branchpoint remain unpaired with a nanocavity at the junction center.[30] Therefore, the overall stability of a nanostructure that includes these junctions depends more on the formation of the *nanostructure*, rather than the stability of the *junction* itself. While significant research has gone into developing more structured nanoassemblies, efforts to gain greater control over the angle of the assembly junctions remain limited.

A significant and recent development to control the angles of nanoassembly junctions was through DNA duplexes strained both in twist and curvature.[7,31] Given that B-form DNA contains about 10.5 base pairs (bp) per turn,[32] DNA sequences designed with more or less bp per turn within a group of helices can alter the pitch/twist and the persistence angle of DNA. However, since the effect arises from single base mismatches, the global structure can only be altered in the long-range. This gives rise to nanostructures that, although bent at the desired angle, are in the order of hundreds of nanometers in length. Such tunable bending of junctions can enable fundamental studies of DNA-binding proteins to bind precisely angled DNA for transcriptional regulation.[31,33] The possibility of angular control within shorter ranges could provide an advantage to build smaller, well-defined architectures. Further, the ability to directly dial in desired angles within a nanostructure would enhance the toolkit for bottom-up designs provided appropriate building blocks were available. Ready angular control of junctions would therefore permit strain free approaches to size- and shape-tunable architectures.

One approach to control junction angles has been through augmenting DNA with synthetic inserts that serve as vertices to orient conjugated DNA strands.[22] Such inserts range from two- and three-armed spacer vertices and transition metal based vertices with diverse coordination geometries, to higher order branched junctions with appropriate building blocks.[12,13,34−42] These require specific *de novo* synthesis of the individual insert for each junction angle thereby posing a high barrier to widespread adoption.

We envision that a more general and versatile alternative to angular control with minimal synthetic inserts can be achieved *directly* through the incorporation of a branch at a specific residue within the sugar−phosphate backbone of duplex B-form DNA. In B-form DNA that has a regular helical twist, the generally accepted pitch arises from 10.5 residues per full turn[32] or 21 residues/base-pairs for two turns of the helix where the 21st residue is directly in line with the first residue. Thus, if branches arose from the helical axis, then the number of residues (*N*) or distance *between* two branches from the backbone would be proportional to the dihedral angle, Θ, between the branches (Figure 1). As the branching junction is on the sugar−phosphate backbone, the branch nucleobases remain free to hybridize into duplexes and the branch can be incorporated directly into sequences within nanostructures. Here, angular control through backbone branching takes advantage of a fundamental feature, the periodicity of the DNA double helix; thus, this is a general and versatile approach that can provide highly tunable control over junction angles.

RESULTS AND DISCUSSION

As proof of this concept, we report the construction of two backbone branched DNA (bbDNA) based nanostructures in which the branches have a dihedral angle of 0° (co-planar branches) and approximately 90° (perpendicular branches). To access such bbDNAs, the synthesis of bbDNA with phosphate linkages directly in the solid-phase[43,44] was initially considered. However, this method would require the specific synthesis of each desired bbDNA individually in the solid-phase with synthetic and yield limitations that hinder practical applications. A more versatile and

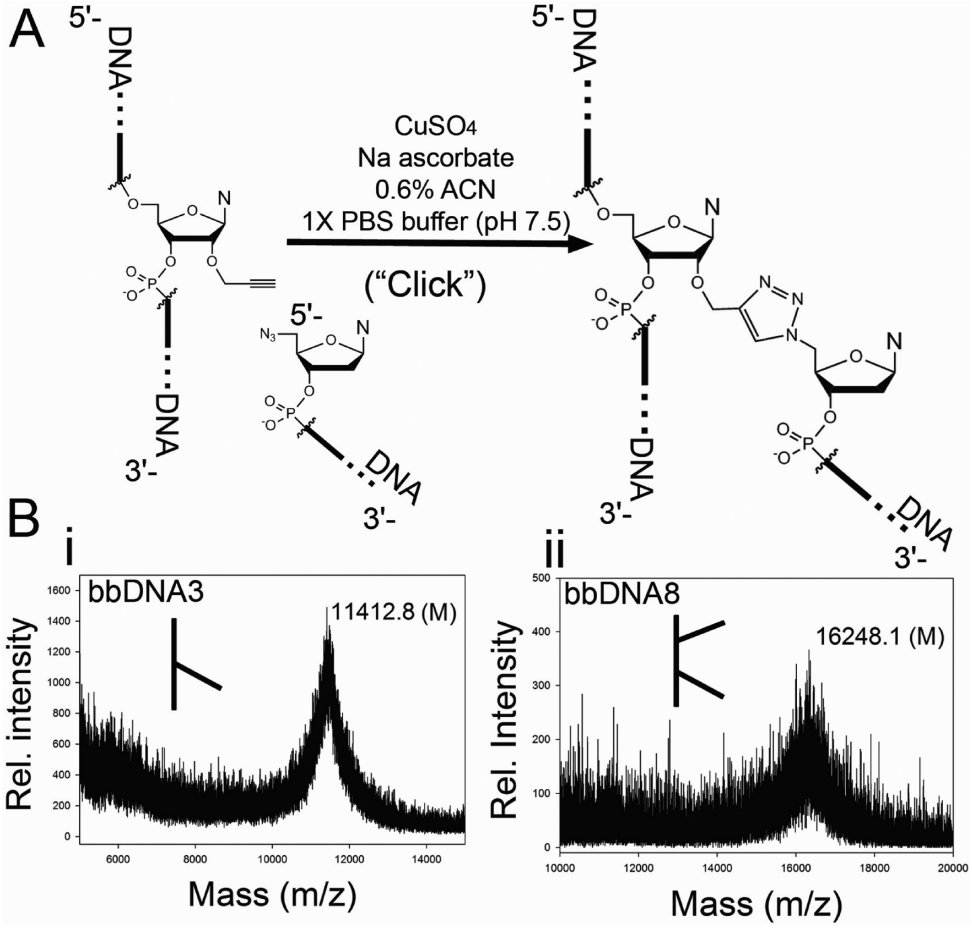

Figure 2. Synthesis of backbone branched DNAs by click chemistry. (A) Click ligation of a 2′-*O*-propargyl DNA with a 5′-azide DNA yields a triazole-linked backbone-branched DNA. (B) MALDI traces of (i) bbDNA3 (with one branch, M_{calc} = 11 413.3) and (ii) bbDNA8 (that includes two branches, M_{calc} = 16 245.5) which show a single mass peak for each respective bbDNA that corresponds closely to the calculated values.

facile post-synthetic branching approach using "click-chemistry" was developed such that these click-bbDNA building blocks are readily accessible in high yield. The bbDNAs form self-assembled nanostructures with expected ladder-like and square tube-like features that were confirmed by gel electrophoresis and visualized by atomic force microscopy (AFM).

The ability to form more structured nanoassemblies with increased angular control through direct backbone modifications within DNA represents an advance over the conventional double crossover and strain promoted junctions and bends used in DNA nanoassemblies. Through control over nanoassembly architecture within such small ranges (20 nt), bbDNAs represent a new building block that significantly expands the design elements and armamentarium for DNA nanotechnology.

Backbone-Branched DNA through "Click-Chemistry". The copper(I)-catalyzed azide–alkyne cycloaddition (CuAAC) reaction, near-synonymous with the term "click-chemistry",[45–48] enjoys widespread use in biomolecular conjugations with proteins, glycans[49–51] and more recently with DNA[52–54] and RNA[55–61] due to its high efficiency. Click-chemistry based DNA building blocks for junctions or assemblies such as circles or hexagons are already enhancing the toolkit for nanoconstruction.[53,62–64] Commercially available 2′-*O*-propargyl phosphoramidites were therefore used to introduce an internal 2′-*O*-propargyl (alkyne) within a DNA sequence (such modified 2′-*O*-alkynyl DNA sequences are also commercially available). With the alkyne in the DNA backbone, it is possible to access bbDNAs by a simple CuAAC reaction with a branch DNA sequence that includes a 5′-terminal azide (Figure 2). The 5′-azide on the DNA is readily installed in the final steps of otherwise standard automated solid-phase DNA synthesis (and such 5′-terminal modification is also commercially available).[65]

Direct CuAAC reactions in aqueous buffer using conditions optimal for terminal nucleic acid conjugation[66,67] were performed between **DNA1** (containing a single internal alkyne) or **DNA7** (containing two internal alkynes) (40 μM) and a 5′-deoxy-5′-azido-**DNA2** (100 μM) to generate triazole-linked **bbDNA3** (that contains a single backbone branch) or **bbDNA8** (that includes two backbone branches) (Figure 2A). To increase the efficiency of the internal click conjugations,

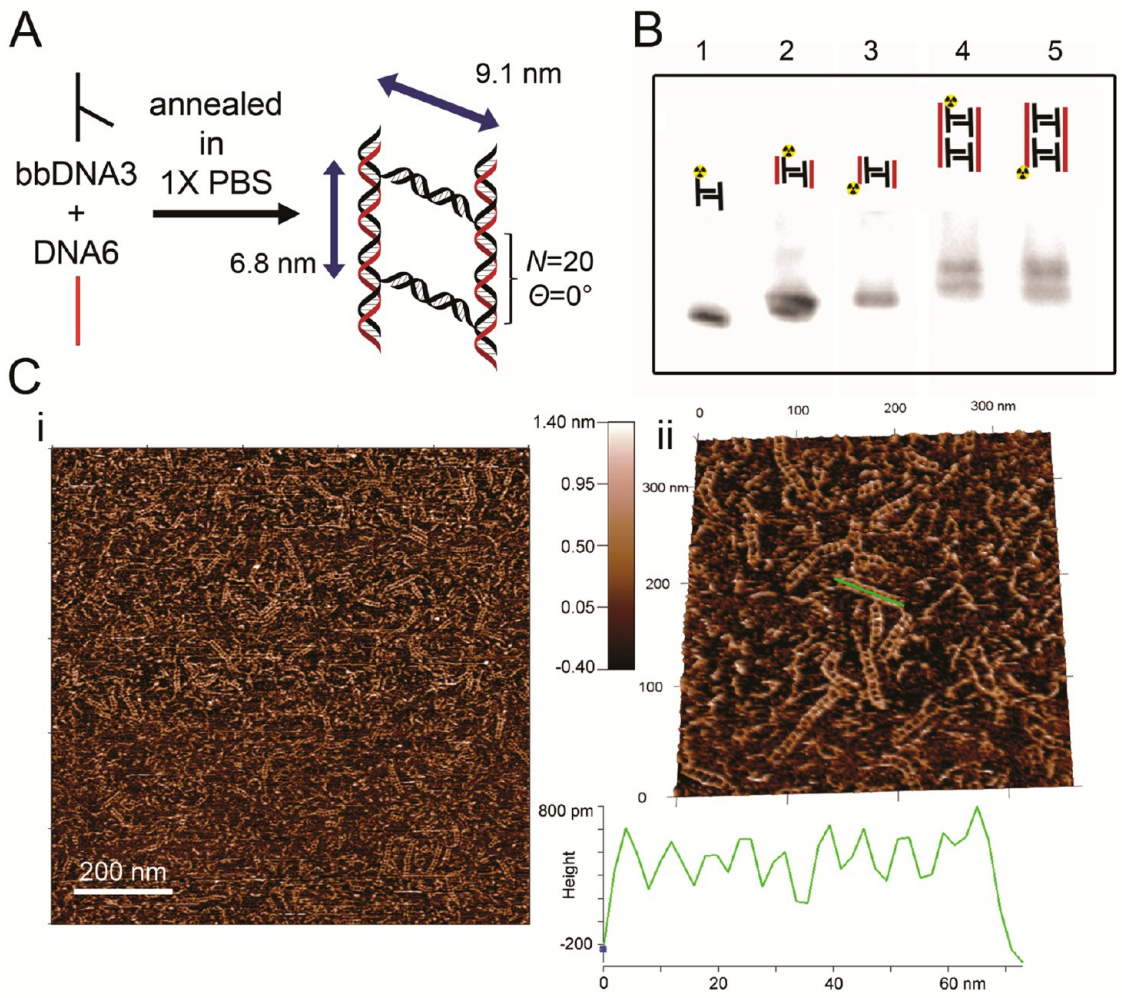

Figure 3. DNA nanoassembly based on co-planar branches. (A) Schematic of annealing of bbDNA3 and DNA6 in 1× PBS to yield a ladder-like nanoassembly in which the number of residues between branches is 20 nts corresponding to a dihedral angle of 0°. (B) Nondenaturing polyacrylamide gel used to resolve annealed building blocks for the ladder-like nanoassembly. Radioactive symbol denotes a trace amount of a 5′-^{32}P-labeled DNA strand that was included. Lane 1: bbDNA3 (the branch is self-complementary). Lanes 2 and 3: Annealed bbDNA3 and DNA4 with the 5′-radiolabel (trace) on either of these DNAs, respectively. Lanes 4 and 5: Annealed bbDNA3 and DNA6 with the 5′-radiolabel (trace) on either of these DNAs, respectively. (C) AFM scan for an assembly of bbDNA3 and DNA5 (that bridges and overhangs) (i) 1 μm × 1 μm square and (ii) zoomed area showing ladder-like nanoassemblies with the line−profile below. See also Supporting Information Figure S3.

the click branching reaction was performed over longer times. The reaction yield was found to be maximal at 3 h with ~80% yield (see Supporting Information). The desired bbDNAs (Figure 2 and Supporting Table S1 for specific sequences) could then be obtained for use in nanostructure assemblies.

Nanoladder Assembly with Co-planar (0°) Branches. The assembly of a nanostructure with a co-planar backbone branch design includes self-complementary branches that are 20 nt apart. With $N = 20$ (where N is the number of residues *between* branches), the 21st residue that includes the second branch will be directly two full helical turns after the first branch and thereby co-planar with a dihedral angle of 0° between the branches. Annealing of **bbDNA3** with sequences **DNA4** or **DNA6** that are complementary to the `stem' (and hybridize with one or two **bbDNA3** stems, respectively) gives rise to higher order structures as observed by (nondenaturing) polyacrylamide gel-shift assays (Figure 3A,B). Regardless of the location of the radioisotopic marker within either **bbDNA3** or the complementary **DNA4** or **DNA6**, bands with similar gel-shift were observed (Figure 2B, lanes 2,3 and 4,5) strongly suggesting that similar complexes were being formed. Annealing of **bbDNA3** with a **DNA5** that is complementary to the stem of **bbBDNA3** but designed to bridge two sequences leaving overhangs, gives rise to larger nanoassemblies confirmed by atomic force microscopy (AFM) imaging. In these images, ladder-like structures are observed (Figure 3C). These ladder-like bbDNA nanostructures have rungs that correspond to the branches that are spaced 6.8 nm on average (from line profiles of $n > 10$ randomly selected visible structures), as may be expected from the design (Table 1).

Square-Tubular Assemblies with Perpendicular (90°) Branches. We next sought nanostructures with two perpendicular

(and identical) branches in which the two self-complementary branches are 20 and 7 nt apart and are expected to have periodic dihedral angles of 0° and approximately 90°, respectively. With $N = 7$, this would correspond to just over three-quarters of a turn or a quarter turn (in the other direction; see Supporting Information Table S2 for dihedral angles between branches). Two crossovers within such short distances (7 nt; a three-quarter turn of the helix) would be strained or frayed and thus the ability of these bbDNAs to form assemblies would represent a demonstrable advantage over crossover and 3WJ based nanoassemblies. A dual-bbDNA is readily achieved by simultaneous click reactions of the branches with a stem that incuded two alkynyl reaction sites at appropriate residues as described above. We tested the ability of this **bbDNA8** with two close branches in assemblies. Annealing of the `stem' of **bbDNA8** with sequences **DNA9** and **DNA11** that are complementary (to one or two strands of **bbDNA8**, respectively) gives rise to higher order structures as observed by gel-shift assays (Figure 4A,B). Annealing of

TABLE 1. Summary of Nanostructure Feature Dimensions As Determined from AFM Images

	structure	
feature	co-planar (ladders)	perpendicular (square-tubes)
Width	~9.7 nm	~20–22.5 nm
Length	50–150 nm	400–1000 nm
Height	1.5 nm	1.5 nm
Inter-rung gap	6.8 ± 0.5 nm	6.4 ± 1 nm

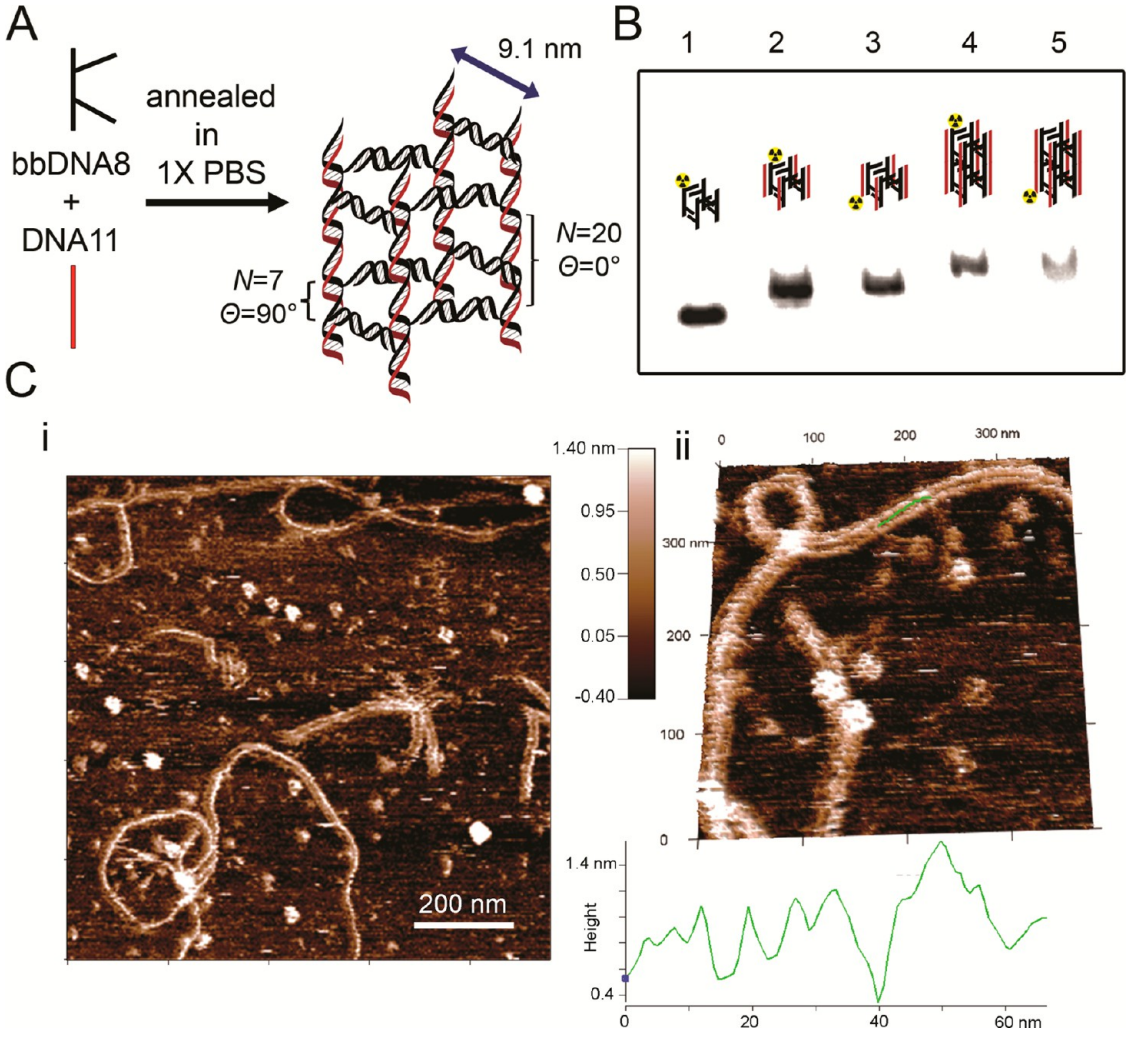

Figure 4. DNA nanoassembly based on dual and perpendicular branches. (A) Schematic of annealing of bbDNA8 and DNA11 in 1× PBS to yield a square prism-like nanoassembly in which the number of residues between branches is 7 and 20 nts corresponding to periodic dihedral angles of nearly 90° and 0°, respectively. (B) Nondenaturing polyacrylamide gel used to resolve annealed building blocks for the square-tube-like nanoassembly. The radioactive symbol denotes a trace amount of a 5′-^{32}P-labeled DNA strand that was included. Lane 1: bbDNA8 (the branches are self-complementary) Lanes 2 and 3: Annealed bbDNA8 and DNA9 with (trace) 5′-radiolabel on one or the other DNA sequence, respectively. Lanes 4 and 5: Annealed bbDNA8 and DNA11 with (trace) 5′-radiolabel on one or the other DNA sequence, respectively. (C) AFM scan for an assembly of bbDNA8 and DNA10 (that includes overhangs) (i) 1 μm × 1 μm square and (ii) zoomed area showing fibrils of square-like tubes with the line–profile below. See also Supporting Information Figure S4.

bbDNA8 with a complementary **DNA10** that bridges two `stems' leaving overhangs gives rise to nanoassemblies confirmed by AFM images in which long fibrils of square tube-like structures are observed (Figure 4C and Table 1). Although the branches were not precisely perpendicular (the theoretical angle is 85.68; see Supporting Information Table S2), the small degree of local flexibility inherent in nucleic acid structure likely compensates. This local flexibility and twisting angles without perfect matches and the length of the interacting helical region is well described and exploited for control of extended angles in multiple array formations.[68] Further, in the bbDNAs here, the oxymethyl-triazole bridge (see Figure 2A) at the branch point may alleviate minor local strain, without sacrificing base-pairing.

To generate useful nanoparticles, it is important that they are thermostable.[69] The consequence of direct extension of a branch sequence from the sugar−phosphate backbone of the helix is mild, having an effect on the melting temperature similar to that of a 2′-*O*-propargyl group (data not shown). While a detailed thermodynamic analysis is forthcoming, the visualization of the bbDNA based structures here and the known stability of base-paired structures in cell lysate[70] suggest that designed structures that incorporate bbDNA would be thermostable. The larger assemblies visualized through AFM rely on overhangs and the thermodynamics of helical stability and overhangs is well described.[69]

CONCLUSIONS

While tremendous advances have been made in the field of DNA nanotechnology, there remain challenges to the design and application of DNA nanostructures, specifically relating to the development of precisely bent architectures.[70] In this report, the highly efficient click-chemistry based synthesis of backbone branched DNAs (bbDNAs) is described. These bbDNAs are building blocks for facile angular control in DNA architectures. Nanostructures with tuned junction angles in the DNA can be obtained readily in high yield (3 h click-branching produces bbDNA in ∼80% yield). These bbDNAs can be designed to self-assemble into two-dimensional ladder-like structures and three-dimensional square tubular nanostructures. In these nanostructures that demonstrate the angular control, the junctions are intrinsically preorganized and the dihedral angles of the assembly are well-defined. While we have demonstrated the use of bbDNAs with the branches on one strand, one can easily envision and design structures where bbDNAs are on both strands of the duplex. Interestingly, as the branch is connected to the 2′-oxygen in a ribosyl residue in the strand, the use of branched nucleic acid building blocks could prove to be useful even within the A-form duplex of RNA. Indeed, recent initiatives take advantage of the diverse folds, structures and thermodynamic stability of RNA for complex and biologically useful architectures.[71−78] The direct angles and twists through bbRNA could form a useful and complementary accessory to the reported strategy. This opens the possibility of exploiting a wide range of angles for branching in the design of three-dimensional nanoconstructs.

Thus click-chemistry based bbNAs represent a new building block for nucleic acids nanotechnology, offering a new and versatile ability to control nanoassembly architecture within small ranges (20 nt). Such bbNAs can directly dial in the required angle in junctions without resorting to crossovers, thereby tremendously simplifying the bottom-up design, size range and access to nanostructures. Internal click reactions on the sugar residue, as shown here with branches, could also be performed on a wide variety of readily available molecules to decorate and functionalize nanostructures.[54,67,79−82]

MATERIALS AND METHODS

Chemicals and General Experimental Information. Commercially available compounds were used without further purification. Phosphoramidites with labile PAC protecting groups and appropriate reagents for standard solid phase synthesis of DNA as well as the 2′-*O*-propargyl phosphoramidite were purchased from ChemGenes. DNA synthesis columns were purchased from Biosearch. Copper sulfate pentahydrate ($CuSO_4 \cdot 5H_2O$) was purchased from Sigma Aldrich. HPLC grade acetonitrile (ACN) was purchased from Fisher. Sodium ascorbate was purchased from Alfa Aesar. Other solvents and reagents not otherwise specified were purchased from Fisher. DNAs were obtained from IDT or synthesized (see below). Matrix assisted laser desorption ionization (MALDI) mass spectra were obtained on an Applied Biosystems Voyager DE-STR MALDI-TOF mass spectrometer.

Oligonucleotide Synthesis and Purification. Solid phase oligonucleotide synthesis was performed on a MerMade 4 instrument (Bioautomation). Synthesis of the oligonucleotides was conducted on commercially available solid support columns and performed with standard commercially available phosphoramidites as directed by the manufacturer. Cleavage from the solid support and base deprotection of the oligonucleotides was performed by using ammonium hydroxide at 65 °C for 2 h and standard protocols for PAC protected amidites as recommended by the manufacturer. Desalting and purification was conducted using a C18 columns (Waters) using protocols recommended by the manufacturer, with elution of the full length desired DNAs with ACN and water. For short sequences as those used here, the coupling efficiency of standard protocols is high and DMT-on purification can remove truncation sequences. As sequences would be gel-purified following the `click'-branching reaction (see below), no prepurification such as HPLC that is recommended was done.

DNA1 and **DNA7** were synthesized using the commercially available 2′-*O*-propargyl phosphoramidite as directed by the manufacturer. **DNA2** was synthesized using standard protocols and the 5′-terminal azide installed on the solid phase by treatment with $(PhO)_3PCH_3I$ (0.5 M in DMF) for 10 min followed by incubation with NaN_3 (sat. in DMF) at 60 °C for 1 h.[60] Where necessary, 5′-end radiolabeling was conducted with T4 PNK using standard protocols. Following radiolabeling, DNAs were purified by electrophoresis on 8 M urea polyacrylamide gels.

The DNA bands were excised and eluted overnight at 4 °C in 10 mM Tris/0.1 mM EDTA ($TE_{0.1}$) buffer (pH 7.5) and desalted using C18 desalting columns (Waters). The DNA sequences synthesized or purchased and used in this study are summarized in Supporting Information Table S1.

Synthesis of Backbone-Branched DNA (bbDNA) *via* Click-Chemistry. A click ligation reaction for branch synthesis was performed with **DNA1** or **DNA7** (40 μM) in 1× PBS (pH 7.5), **DNA2** (100 μM), sodium ascorbate (5 mM) and ACN (0.6%). The reaction mixture was degassed and the reaction was initiated by the addition of $CuSO_4$ (400 μM) and allowed to run for 1 h under argon at room temperature with shaking. The reaction mixture was loaded on a 10% polyacrylamide gel (8 M urea) to stop the reaction, resolve and visualize the DNAs (Supporting Information Figure S1). The DNA bands were excised, eluted and desalted as before. Mass spectra confirm the synthesis of the two desired branches with corresponding masses of 11 412.8 (M) for **bbDNA3** and 16 248.1(M) for **bbDNA8** (Masses calculated are 11 413.3 and 16 245.5, respectively; see Figure 2B)

Optimizing Timing for the Backbone-Branching Click-Reaction. The click reactions for bbDNA synthesis were performed with **DNA1** (3 μM) that included trace amounts of 5′-^{32}P radiolabel in 1× PBS (pH 7.5), **DNA2** (10 μM), sodium ascorbate (150 μM) and ACN (0.6%).[66] The reaction mixture was degassed (by argon displacement) and the reaction was initiated by the addition of $CuSO_4$ (30 μM) and allowed to run for 0, 0.25, 0.5, 1, 1.5, 2, 3, or 5 h under argon at room temperature with shaking to yield **bbDNA3**. The reaction mixtures were directly loaded and run on a denaturing 20% polyacrylamide gel (8 M urea) to stop the reaction, and resolve DNAs. The dried gel was exposed to phosphor screen and imaged on a Storm phosphorimager (Molecular Dynamics). The reaction products were quantified and normalized to the sum of the product (**bbDNA3**) and starting material (**DNA1**) bands with ImageQuant software (see Supporting Information Figure S1).

Gel-Shift Assays to Observe Hybridization of bbDNA. A solution of **bbDNA3** or **bbDNA8** (3 μM) and **DNA 4**/**DNA6** or **DNA9**/**DNA11** (3 μM), respectively, with trace amounts of ^{32}P labeled DNAs as mentioned, in 1× PBS and 2.5 mM $MgCl_2$ was heated to 95 °C for 2 min and cooled in a stepwise manner (see Supporting Information Figure S2). Following annealing, the solutions were kept at 4 °C for 10 min prior to loading on a 10% nondenaturing polyacrylamide gel run at 4 °C for nanoassembly resolution. The dried gels were exposed to a phosphor screen and imaged on a Storm phosphorimager (Molecular Dynamics).

Nanoassembly Formation and AFM Imaging. A 10 μL solution of 1× PBS buffer with 25 ng of **bbDNA3** or **bbDNA8** and 25 ng of **DNA5** or **DNA10**, respectively, were annealed as before. The branched strand (200 nM) and complement strand were mixed in 1× PBS buffer in a molar ratio of 1:1 or 3:1. DNA assembly was formed by similar protocols as described earlier.[83,84] The mixture was heated at 95 °C for 3 min, and then the assembly was formed by slowly cooling down to 4 °C in 48 h. DNA assembly samples were directly used after assembly for AFM imaging, without any further purification or isolation. AFM imaging of the nanostructures was conducted on flat mica surfaces. To immobilize the DNA assembly to the mica, the surface was treated with 3-aminopropyltriethoxysilane (APTES) to form a net positively charged aminopropyl-mica (AP-mica), which can immobilize negatively charged DNA. Freshly cleaved mica was incubated in the vapor of 3-aminopropyltriethoxysilane (APTES) in a vacuum desiccator for 2 h.[85] Following the surface functionalization, 2 μL of 10× diluted solution was deposited for 2 min. Surfaces were rinsed with PBS buffer to remove any unbound DNA assembly. Imaging was conducted in solution (PBS buffer) in noncontact mode using an Asylum MFP-3D AFM (Asylum Research, Santa Barbara, CA). Super sharp CSG cantilevers from NT-MDT (Moscow, Russia) and SNL cantilevers from Bruker (Camarillo, CA) were used for AFM imaging. These cantilevers with nominal radii of curvature ~5 nm were used to provide high resolution images of the sub-50 nm assemblies.

Conflict of Interest: The authors declare no competing financial interest.

Supporting Information Available: The specific DNA sequences used, gel images and optimization of click-reaction timing, time−temperature trace for annealing protocol for nanoassembly, a table of expected angles from branching and additional AFM images of assemblies. This material is available free of charge *via* the Internet at http://pubs.acs.org.

Acknowledgment. E.P. and S.R.D. wish to acknowledge the Department of Chemistry at Carnegie Mellon University for start-up funds and the DSF Charitable Foundation for additional funding. V.K.Y. wishes to acknowledge Thomas F. and Kate Miller Jeffress Memorial Trust for partial support. We thank T. Kowaleski and B. Van Houten for helpful discussions and advice.

REFERENCES AND NOTES

1. Seeman, N. C. Nucleic-Acid Junctions and Lattices. *J. Theor. Biol.* **1982**, *99*, 237–247.
2. Kallenbach, N. R.; Ma, R. I.; Seeman, N. C. An Immobile Nucleic-Acid Junction Constructed from Oligonucleotides. *Nature* **1983**, *305*, 829–831.
3. Chen, J. H.; Seeman, N. C. Synthesis from DNA of a Molecule with the Connectivity of a Cube. *Nature* **1991**, *350*, 631–633.
4. Winfree, E.; Liu, F. R.; Wenzler, L. A.; Seeman, N. C. Design and Self-assembly of Two-Dimensional DNA Crystals. *Nature* **1998**, *394*, 539–544.
5. Zheng, J. P.; Birktoft, J. J.; Chen, Y.; Wang, T.; Sha, R. J.; Constantinou, P. E.; Ginell, S. L.; Mao, C. D.; Seeman, N. C. From Molecular to Macroscopic *via* the Rational Design of a Self-assembled 3D DNA Crystal. *Nature* **2009**, *461*, 74–77.
6. Seeman, N. C. Nanomaterials Based on DNA. *Annu. Rev. Biochem.* **2010**, *79*, 65–87.
7. Torring, T.; Voigt, N. V; Nangreave, J.; Yan, H.; Gothelf, K. V DNA Origami: A Quantum Leap for Self-Assembly of Complex Structures. *Chem. Soc. Rev.* **2011**, *40*, 5636–5646.
8. Rothemund, P. W. K. Folding DNA To Create Nanoscale Shapes and Patterns. *Nature* **2006**, *440*, 297–302.
9. Li, Y. G.; Tseng, Y. D.; Kwon, S. Y.; D'Espaux, L.; Bunch, J. S.; Mceuen, P. L.; Luo, D. Controlled Assembly of Dendrimer-like DNA. *Nat. Mater.* **2004**, *3*, 38–42.
10. Shih, W. M.; Quispe, J. D.; Joyce, G. F. A 1.7-kilobase Single-stranded DNA That Folds into a Nanoscale Octahedron. *Nature* **2004**, *427*, 618–621.
11. Lin, C. X.; Liu, Y.; Rinker, S.; Yan, H. DNA Tile Based Self-assembly: Building Complex Nanoarchitectures. *ChemPhyschem* **2006**, *7*, 1641–1647.
12. Aldaye, F. A.; Sleiman, H. F. Guest-mediated Access to a Single DNA Nanostructure from a Library of Multiple Assemblies. *J. Am. Chem. Soc.* **2007**, *129*, 10070–10071.
13. Aldaye, F. A.; Sleiman, H. F. Modular Access to Structurally Switchable 3D Discrete DNA Assemblies. *J. Am. Chem. Soc.* **2007**, *129*, 13376–13377.
14. Andersen, E. S.; Dong, M. D.; Nielsen, M. M.; Jahn, K.; Lind-Thomsen, A.; Mamdouh, W.; Gothelf, K. V; Besenbacher, F.; Kjems, J. DNA Origami Design of Dolphin-shaped Structures with Flexible Tails. *ACS Nano* **2008**, *2*, 1213–1218.
15. Andersen, E. S.; Dong, M.; Nielsen, M. M.; Jahn, K.; Subramani, R.; Mamdouh, W.; Golas, M. M.; Sander, B.; Stark, H.; Oliveira, C. L. P.; *et al.* Self-assembly of a Nanoscale DNA Box with a Controllable Lid. *Nature* **2009**, *459*, 73–76.
16. Douglas, S. M.; Marblestone, A. H.; Teerapittayanon, S.; Vazquez, A.; Church, G. M.; Shih, W. M. Rapid Prototyping of 3D DNA-origami Shapes with caDNAno. *Nucleic Acids Res.* **2009**, *37*, 5001–5006.
17. Kuzuya, A.; Komiyama, M. Design and Construction of a Box-shaped 3D-DNA Origami. *Chem. Commun.* **2009**, 4182–4184.
18. Endo, M.; Hidaka, K.; Kato, T.; Namba, K.; Sugiyama, H. DNA Prism Structures Constructed by Folding of Multiple Rectangular Arms. *J. Am. Chem. Soc.* **2009**, *131*, 15570–15571.
19. Bhatia, D.; Mehtab, S.; Krishnan, R.; Indi, S. S.; Basu, A.; Krishnan, Y. Icosahedral DNA Nanocapsules by Modular Assembly. *Angew. Chem., Int. Ed.* **2009**, *48*, 4134–4137.
20. Ke, Y. G.; Sharma, J.; Liu, M. H.; Jahn, K.; Liu, Y.; Yan, H. Scaffolded DNA Origami of a DNA Tetrahedron Molecular Container. *Nano Lett.* **2009**, *9*, 2445–2447.

21. Han, D. R.; Pal, S.; Nangreave, J.; Deng, Z. T.; Liu, Y.; Yan, H. DNA Origami with Complex Curvatures in Three-Dimensional Space. *Science* **2011**, *332*, 342–346.
22. McLaughlin, C. K.; Hamblin, G. D.; Sleiman, H. F. Supramolecular DNA Assembly. *Chem. Soc. Rev.* **2011**, *40*, 5647–5656.
23. Keller, S.; Marx, A. The Use of Enzymes for Construction of DNA-Based Objects and Assemblies. *Chem. Soc. Rev.* **2011**, *40*, 5690–5697.
24. Sacca, B.; Niemeyer, C. M. Functionalization of DNA Nanostructures with Proteins. *Chem. Soc. Rev.* **2011**, *40*, 5910–5921.
25. Wei, B.; Dai, M.; Yin, P. Complex Shapes Self-Assembled from Single-Stranded DNA Tiles. *Nature* **2012**, *485*, 623–626.
26. Walsh, A. S.; Yin, H.; Erben, C. M.; Wood, M. J. A.; Turberfield, A. J. DNA Cage Delivery to Mammalian Cells. *ACS Nano* **2011**, *5*, 5427–5427.
27. Ozhalici-Unal, H.; Armitage, B. A. Fluorescent DNA Nanotags Based on a Self-Assembled DNA Tetrahedron. *ACS Nano* **2009**, *3*, 425–433.
28. Bhatia, D.; Surana, S.; Chakraborty, S.; Koushika, S. P.; Krishnan, Y. A Synthetic Icosahedral DNA-Based Host–Cargo Complex for Functional *in Vivo* Imaging. *Nat. Commun.* **2011**, *2*, 339.
29. Lee, H.; Lytton-Jean, A. K.; Chen, Y.; Love, K. T.; Park, A. I.; Karagiannis, E. D.; Sehgal, A.; Querbes, W.; Zurenko, C. S.; Jayaraman, M.; *et al.* Molecularly Self-assembled Nucleic Acid Nanoparticles for Targeted *in Vivo* siRNA Delivery. *Nat. Nanotechnol.* **2012**, *7*, 389–393.
30. Sabir, T.; Toulmin, A.; Ma, L.; Jones, A. C.; McGlynn, P.; Schröder, G. F.; Magennis, S. W. Branchpoint Expansion in a Fully Complementary Three-Way DNA Junction. *J. Am. Chem. Soc.* **2012**, *134*, 6280–6285.
31. Dietz, H.; Douglas, S. M.; Shih, W. M. Folding DNA into Twisted and Curved Nanoscale Shapes. *Science* **2009**, *325*, 725–730.
32. Klug, A.; Rhodes, D. Sequence-Dependent Helical Periodicity of DNA. *Nature* **1981**, *292*, 378–380.
33. Parker, S. C. J.; Hansen, L.; Abaan, H. O.; Tullius, T. D.; Margulies, E. H.; Local, D. N. A. Topography Correlates with Functional Noncoding Regions of the Human Genome. *Science* **2009**, *324*, 389–392.
34. Seeman, N. C.; Kallenbach, N. R. DNA Branched Junctions. *Ann. Rev. Biophys. Biomol. Struct.* **1994**, *23*, 53–86.
35. Shi, J.; Bergstrom, D. E. Assembly of Novel DNA Cycles with Rigid Tetrahedral Linkers. *Angew. Chem., Int. Ed.* **1997**, *36*, 111–113.
36. Stewart, K. M.; Rojo, J.; McLaughlin, L. W. Ru(II) Tris-(bipyridyl) Complexes with Six Oligonucleotide Arms as Precursors for the Generation of Supramolecular Assemblies. *Angew. Chem., Int. Ed.* **2004**, *43*, 5808–5811.
37. Endo, M.; Seeman, N. C.; Majima, T. DNA Tube Structures Controlled by a Four-Way-Branched DNA Connector. *Angew. Chem., Int. Ed.* **2005**, *44*, 6074–6077.
38. Vargas-Baca, I.; Mitra, D.; Zulyniak, H. J.; Banerjee, J.; Sleiman, H. F. Solid-Phase Synthesis of Transition Metal Linked, Branched Oligonucleotides. *Angew. Chem., Int. Ed.* **2001**, *40*, 4629–4632.
39. Mitra, D.; Di Cesare, N.; Sleiman, H. F. Self-Assembly of Cyclic Metal–DNA Nanostructures Using Ruthenium Tris-(bipyridine)-Branched Oligonucleotides. *Angew. Chem., Int. Ed.* **2004**, *43*, 5804–5808.
40. Yang, H.; Sleiman, H. F. Templated Synthesis of Highly Stable, Electroactive, and Dynamic Metal–DNA Branched Junctions. *Angew. Chem., Int. Ed.* **2008**, *47*, 2443–2446.
41. Yang, H.; Altvater, F.; de Bruijn, A. D.; McLaughlin, C. K.; Lo, P. K.; Sleiman, H. F. Chiral Metal–DNA Four-Arm Junctions and Metalated Nanotubular Structures. *Angew. Chem., Int. Ed.* **2011**, *50*, 4620–4623.
42. Lee, J. K.; Jung, Y. H.; Tok, J. B. H.; Bao, Z. Syntheses of Organic Molecule–DNA Hybrid Structures. *ACS Nano* **2011**, *5*, 2067–2074.
43. Damha, M. J.; Zabarylo, S. Automated Solid-Phase Synthesis of Branched Oligonucleotides. *Tetrahedron Lett.* **1989**, *30*, 6295–6298.
44. Carriero, S.; Damha, M. J. Solid-Phase Synthesis of Branched Oligonucleotides. In *Current Protocs in Nucleic Acid Chemistry*; John Wiley & Sons, Inc.: New York, 2002; Unit 4.14; pp 4.14.1–4.14.32.
45. Kolb, H. C.; Finn, M. G.; Sharpless, K. B. Click Chemistry: Diverse Chemical Function from a Few Good Reactions. *Angew. Chem., Int. Ed.* **2001**, *40*, 2004–2021.
46. Tornøe, C. W.; Christensen, C.; Meldal, M. Peptidotriazoles on Solid Phase: [1,2,3]-Triazoles by Regiospecific Copper-(I)-Catalyzed 1,3-Dipolar Cycloadditions of Terminal Alkynes to Azides. *J. Org. Chem.* **2002**, *67*, 3057–3064.
47. Rostovtsev, V. V; Green, L. G.; Fokin, V. V; Sharpless, K. B. A Stepwise Huisgen Cycloaddition Process: Copper(I)-Catalyzed Regioselective "Ligation" of Azides and Terminal Alkynes. *Angew. Chem., Int. Ed.* **2002**, *41*, 2596–2599.
48. Finn, M. G.; Fokin, V. Click Chemistry: Function Follows Form. *Chem. Soc. Rev.* **2010**, *39*, 1231–1232.
49. Best, M. D. Click Chemistry and Bioorthogonal Reactions: Unprecedented Selectivity in the Labeling of Biological Molecules. *Biochemistry* **2009**, *48*, 6571–6584.
50. Sletten, E. M.; Bertozzi, C. R. Bioorthogonal Chemistry: Fishing for Selectivity in a Sea of Functionality. *Angew. Chem., Int. Ed.* **2009**, *48*, 6974–6998.
51. Mamidyala, S. K.; Finn, M. G. *In Situ* Click Chemistry: Probing the Binding Landscapes of Biological Molecules. *Chem. Soc. Rev.* **2010**, *39*, 1252–1261.
52. El-Sagheer, A. H.; Brown, T. Click Chemistry with DNA. *Chem. Soc. Rev.* **2010**, *39*, 1388–1405.
53. Gerrard, S. R.; Hardiman, C.; Shelbourne, M.; Nandhakumar, I.; Nordén, B.; Brown, T. A New Modular Approach to Nanoassembly: Stable and Addressable DNA Nanoconstructs *via* Orthogonal Click Chemistries. *ACS Nano* **2012**, *6*, 9221–9228.
54. Gierlich, J.; Burley, G. A.; Gramlich, P. M. E.; Hammond, D. M.; Carell, T. Click Chemistry as a Reliable Method for the High-Density Postsynthetic Functionalization of Alkyne-Modified DNA. *Org. Lett.* **2006**, *8*, 3639–3642.
55. El-Sagheer, A. H.; Brown, T. New Strategy for the Synthesis of Chemically Modified RNA Constructs Exemplified by Hairpin and Hammerhead Ribozymes. *Proc. Natl. Acad. Sci. U.S.A.* **2010**, *107*, 15329–15334.
56. Paredes, E.; Das, S. R. Click Chemistry for Rapid Labeling and Ligation of RNA. *ChemBioChem* **2011**, *12*, 125–131.
57. Aigner, M.; Hartl, M.; Fauster, K.; Steger, J.; Bister, K.; Micura, R. Chemical Synthesis of Site-Specifically 2'-Azido-Modified RNA and Potential Applications for Bioconjugation of siRNA Technologies. *ChemBioChem* **2011**, *12*, 47–51.
58. Kellner, S.; Seidu-Larry, S.; Burhenne, J.; Motorin, Y.; Helm, M. A Multifunctional Bioconjugate Module for Versatile Photoaffinity Labeling and Click Chemistry of RNA. *Nucleic Acids Res.* **2011**, *39*, 7348–7360.
59. Peacock, H.; Maydanovych, O.; Beal, P. A. N^2-Modified 2-Aminopurine Ribonucleosides as Minor-Groove-Modulating Adenosine Replacements in Duplex RNA. *Org. Lett.* **2010**, *12*, 1044–1047.
60. Winz, M.-L.; Samanta, A.; Benzinger, D.; Jäschke, A. Site-Specific Terminal and Internal Labeling of RNA by poly(A) Polymerase Tailing and Copper-Catalyzed or Copper-Free Strain-Promoted Click Chemistry. *Nucleic Acids Res.* **2012**, *40*, e78.
61. Hong, V.; Presolski, S. I.; Ma, C.; Finn, M. G. Analysis and Optimization of Copper-Catalyzed Azide-Alkyne Cycloaddition for Bioconjugation. *Angew. Chem., Int. Ed.* **2009**, *48*, 9879–9883.
62. Lundberg, E. P.; El-Sagheer, A. H.; Kocalka, P.; Wilhelmsson, L. M.; Brown, T.; Norden, B. A New Fixation Strategy for Addressable Nano-network Building Blocks. *Chem. Commun.* **2010**, *46*, 3714–3716.
63. Lundberg, E. P.; Plesa, C.; Wilhelmsson, L. M.; Lincoln, P.; Brown, T.; Nordén, B. Nanofabrication Yields. Hybridization and Click-Fixation of Polycyclic DNA Nanoassemblies. *ACS Nano* **2011**, *5*, 7565–7575.
64. Kumar, R.; El-Sagheer, A.; Tumpane, J.; Lincoln, P.; Wilhelmsson, L. M.; Brown, T. Template-Directed Oligonucleotide Strand

Ligation, Covalent Intramolecular DNA Circularization and Catenation Using Click Chemistry. *J. Am. Chem. Soc.* **2007**, *129*, 6859–6864.
65. Miller, G. P.; Kool, E. T. Versatile 5′-Functionalization of Oligonucleotides on Solid Support: Amines, Azides, Thiols, and Thioethers *via* Phosphorus Chemistry. *J. Org. Chem.* **2004**, *69*, 2404–2410.
66. Paredes, E.; Das, S. R. Optimization of Acetonitrile Co-solvent and Copper Stoichiometry for Pseudo-Ligandless Click Chemistry with Nucleic Acids. *Bioorg. Med. Chem. Lett.* **2012**, *22*, 5313–5316.
67. Averick, S. E.; Paredes, E.; Grahacharya, D.; Woodman, B. F.; Miyake-Stoner, S. J.; Mehl, R. A.; Matyjaszewski, K.; Das, S. R. A Protein−Polymer Hybrid Mediated By DNA. *Langmuir* **2012**, *28*, 1954–1958.
68. Shu, D.; Moll, W.-D.; Deng, Z.; Mao, C.; Guo, P. Bottom-up Assembly of RNA Arrays and Superstructures as Potential Parts in Nanotechnology. *Nano Lett.* **2011**, *6*, 763–772.
69. Guo, P. The Emerging Field of RNA Nanotechnology. *Nat. Nanotechnol.* **2010**, *5*, 833–842.
70. Mei, Q.; Wei, X.; Su, F.; Liu, Y.; Youngbull, C.; Johnson, R.; Lindsay, S.; Yan, H.; Meldrum, D. Stability of DNA Origami Nanoarrays in Cell Lysate. *Nano Lett.* **2011**, *11*, 1477–1482.
71. Pinheiro, A. V; Han, D.; Shih, W. M.; Yan, H. Challenges and Opportunities for Structural DNA Nanotechnology. *Nat. Nanotechnol.* **2011**, *6*, 763–772.
72. Shukla, G. C.; Haque, F.; Tor, Y.; Wilhelmsson, L. M.; Toulmé, J.-J.; Isambert, H.; Guo, P.; Rossi, J. J.; Tenenbaum, S. A.; Shapiro, B. A. A Boost for the Emerging Field of RNA Nanotechnology. *ACS Nano* **2011**, *5*, 3405–3418.
73. Krishnan, Y.; Simmel, F. C. Nucleic Acid Based Molecular Devices. *Angew. Chem., Int. Ed.* **2011**, *50*, 3124–3156.
74. Krishnan, Y.; Bathe, M. Designer Nucleic Acids to Probe and Program the Cell. *Trends Cell Biol.* **2012**, *22*, 624–633.
75. Jaeger, L.; Chworos, A. The Architectonics of Programmable RNA and DNA Nanostructures. *Curr. Opin. Struct. Biol.* **2006**, *16*, 531–543.
76. Shu, D.; Shu, Y.; Haque, F.; Abdelmawla, S.; Guo, P. Thermodynamically Stable RNA Three-Way Junction for Constructing Multifunctional Nanoparticles for Delivery of Therapeutics. *Nat. Nanotechnol.* **2011**, *6*, 658–667.
77. Dibrov, S. M.; McLean, J.; Parsons, J.; Hermann, T. Self-Assembling RNA Square. *Proc. Natl. Acad. Sci. U.S.A.* **2011**, *108*, 6405–6408.
78. Mei, Q.; Wei, X.; Su, F.; Liu, Y.; Youngbull, C.; Johnson, R.; Lindsay, S.; Yan, H.; Meldrum, D. Stability of DNA Origami Nanoarrays in Cell Lysate. *Nano Lett.* **2011**, *11*, 1477–1482.
79. Averick, S.; Paredes, E.; Li, W.; Matyjaszewski, K.; Das, S. R. Direct DNA Conjugation to Star Polymers for Controlled Reversible Assemblies. *Bioconjugate Chem.* **2011**, *22*, 2030–2037.
80. Fischler, M.; Sologubenko, A.; Mayer, J.; Clever, G.; Burley, G.; Gierlich, J.; Carell, T.; Simon, U. Chain-like Assembly of Gold Nanoparticles on Artificial DNA Templates *via* "Click Chemistry. *Chem. Commun* **2008**, 169–171.
81. Gramlich, P. M. E.; Warncke, S.; Gierlich, J.; Carell, T. Click-Click-Click: Single to Triple Modification of DNA. *Angew. Chem., Int. Ed.* **2008**, *47*, 3442–3444.
82. Zhang, X. J.; Yadavalli, V. K. Functional Self-Assembled DNA Nanostructures for Molecular Recognition. *Nanoscale* **2012**, *4*, 2439–2446.
83. Park, S. H.; Yin, P.; Liu, Y.; Reif, J. H.; LaBean, T. H.; Yan, H. Programmable DNA Self-Assemblies for Nanoscale Organization of Ligands and Proteins. *Nano Lett.* **2005**, *5*, 729–733.
84. He, Y.; Tian, Y.; Ribbe, A. E.; Mao, C. Antibody Nanoarrays with a Pitch of Approximately 20 Nanometers. *J. Am. Chem. Soc.* **2006**, *128*, 12664–12665.
85. Lyubchenko, Y. L.; Gall, A. A.; Shlyakhtenko, L. S.; Harrington, R. E.; Jacobs, B. L.; Oden, P. I.; Lindsay, S. M. Atomic Force Microscopy Imaging of Double Stranded DNA and RNA. *J. Biomol. Struct Dyn.* **1992**, *10*, 589–606.